

NONLINEAR HIGHER-ORDER LABEL SPREADING

Francesco Tudisco
School of Mathematics
Gran Sasso Science Institute
67100, L'Aquila Italy
francesco.tudisco@gssi.it

Austin R. Benson
Department of Computer Science
Cornell University
Ithaca, NY 14853
arb@cs.cornell.edu

Konstantin Prokopchik
School of Computer Science
Gran Sasso Science Institute
67100, L'Aquila Italy
konstantin.prokopchik@gssi.it

ABSTRACT

Label spreading is a general technique for semi-supervised learning with point cloud or network data, which can be interpreted as a diffusion of labels on a graph. While there are many variants of label spreading, nearly all of them are linear models, where the incoming information to a node is a weighted sum of information from neighboring nodes. Here, we add nonlinearity to label spreading through nonlinear functions of higher-order structure in the graph, namely triangles in the graph. For a broad class of nonlinear functions, we prove convergence of our nonlinear higher-order label spreading algorithm to the global solution of a constrained semi-supervised loss function. We demonstrate the efficiency and efficacy of our approach on a variety of point cloud and network datasets, where the nonlinear higher-order model compares favorably to classical label spreading, as well as hypergraph models and graph neural networks.

1 Introduction

Label Spreading (LS) is a general algorithmic technique for Semi-Supervised Learning (SSL), where one infers unknown labels from known labels by iteratively diffusing or “spreading” the known labels over a similarity graph where nodes correspond to data points and are connected by edges if they are similar [62]. With generic point cloud data, edges are typically k -nearest-neighbors or ϵ -neighbors [28, 59, 61], but LS can also be used directly on relational data coming from, e.g., social networks [13], web graphs [32], or co-purchases [21]. A canonical or “standard” implementation of label spreading is the iterative local and global consistency approach [59]. In this method, nodes iteratively spread their current label to neighbors (encouraging local consistency), and originally labeled points try to remain close to their initial labels (encouraging global consistency). This procedure corresponds to a linear gradient-flow that minimizes a regularized loss function in the limit.

The linearity of the diffusion makes standard LS simple to implement. From the perspective of an unlabeled data point, the corresponding node in the graph iteratively updates its label based on a fixed *linear* combination (the mean) of the current labels of its neighbors in the graph. The linearity also makes it easy to analyze the limiting behavior of this iterative process, which coincides with the solution of a Laplacian linear system. At the same time, nonlinear methods provide stronger modeling capabilities, making them a hallmark of deep learning [22] and kernel methods [25].

Here, we incorporate nonlinearity into label spreading via nonlinear functions on so-called “higher-order” relationships between the data points, i.e., information about groups of nodes instead of just the similarities encoded by edges in a graph. More specifically, we use a similarity *hypergraph* that encodes higher-order relationships. This hypergraph can come directly from data or be derived from a similarity graph (we often use the hypergraph induced by the 3-cliques in a similarity graph). From this, we devise a new spreading process, where a given node u updates its label based on the labels of the other nodes in the hyperedges that contain u . Importantly, we allow the spreading of information at a hyperedge to be any of a broad class of nonlinear “mixing functions.”

We call our approach Nonlinear Higher-Order Label Spreading (NHOLS) since it uses both nonlinear and higher-order information. Even though the nonlinearity of our spreading process makes analysis more challenging, we show that NHOLS enjoys several nice properties similar to standard LS. First, NHOLS minimizes a regularized loss function which combines a global consistency term with a higher-order local consistency term. Second, for a broad class of nonlinear mixing functions, NHOLS globally converges to a unique global minimizer of this loss function. Furthermore, in terms of implementation, NHOLS shares the same simplicity and efficiency as standard LS. Each iteration only requires a single pass over the input data, making it highly scalable.

We evaluate NHOLS on a number of synthetic and real-world datasets, comparing against standard LS, hypergraph semi-supervised learning methods, and graph neural networks. We find that incorporating nonlinearities of higher-

order information into label spreading almost always achieves the best performance, while also being nearly as fast as standard LS.

1.1 Related work

Higher-order information for graph data. A key idea in many recent graph-based learning methods is that incorporating *higher-order* interactions involving multiple nodes can make large changes in performance. This has yielded improvements in numerous settings, including unsupervised clustering [10, 36, 50], localized clustering [35, 57], representation learning [44], link prediction [6, 9, 45], graph classification [2], ranking [6, 7, 8, 14], and data visualization [42]. A higher-order version of label spreading has also recently been developed for relational data [16], and this correspond to the special case of linear mixing functions within our framework.

Hypergraph learning. There are many machine learning methods for hypergraph data, and a standard approach is to first reduce the hypergraph to a graph upon which a graph-based method can be employed [1, 17, 36, 46, 58, 60]. These techniques are “clique expansions”, as they place a (possibly weighted) clique in the graph for every hyperedge. Using a linear mixing function in our framework is a clique expansion technique, which we cover in Section 3. Our analysis is focused on nonlinear mixing functions, which is not a clique expansion. Thus, our framework is conceptually closer to hypergraph methods that avoid clique expansions, such as those based on nonlinear Hypergraph Laplacian operators [12, 37, 56] or generalized splitting functions [51, 52].

Nonlinear semi-supervised learning. There are variants of label spreading techniques that use nonlinearities, such as p -Laplacians [3, 11, 26] and their limits [32]. Our theoretical framework provides new convergence guarantees for some of these approaches.

Tensor methods. Tensors can also represent higher-order data and are broadly used in machine learning [5, 27, 43, 47, 53]. We analyze the iterations of NHOLS as a type of tensor contraction; from this, we extend recent nonlinear Perron-Frobenius theory [19, 20] to establish convergence results.

2 Background on Standard Label Spreading

We first review a “standard” LS technique that is essentially the same as the one of Zhou et al. [59] so that we can later draw parallels with our new nonlinear higher-order method. Let $G = (V, E, \omega)$ be a weighted undirected graph with nodes $V = \{1, \dots, n\}$, edge set $E \subseteq V \times V$ and edge-weight function $\omega(ij) > 0$. As mentioned in the introduction, G typically represents either a similarity graph for a point cloud or a bona fide relational network. Let A be the adjacency matrix of G , i.e., by $A_{ij} = \omega(ij)$ if $ij \in E$ and $A_{ij} = 0$ otherwise. Furthermore, let $D_G = \text{Diag}(d_1, \dots, d_n)$ be the diagonal degree matrix of G , where $d_i = \sum_j A_{ij}$. Throughout this paper, we will assume that G has no isolated nodes, that is D_G has no zero diagonal entries. Finally, let $S = D_G^{-1/2} A D_G^{-1/2}$ be the normalized adjacency matrix.

Our goal is to provide a label in $\{1, \dots, L\}$ to each node, and we know the label of (usually a small) subset of the nodes. The initial labels are represented by membership vectors in an $n \times c$ matrix Y , where $Y_{i,\ell} = 1$ if node i has initial label ℓ and $Y_{i,\ell} = 0$ otherwise. Given an initial guess $F^{(0)} \in \mathbb{R}^{n \times c}$, the label spreading algorithm iteratively computes

$$F^{(r+1)} = \beta S F^{(r)} + \gamma Y \quad r = 0, 1, 2, \dots, \quad (1)$$

with $\beta, \gamma \geq 0$ and $\beta + \gamma = 1$. The iterates converge to the solution of the linear system $(I - \beta S)F^* = \gamma Y$, but in practice, a few iterations of (1) with the initial point $F^{(0)} = Y$ suffices [18]. This yields an approximate solution \tilde{F}^* . The prediction on an unlabeled node j is then $\arg \max_{\ell} \tilde{F}_{j,\ell}^*$. Also, in practice, one can perform this iteration column-wise with one initial vector y per label class.

The label spreading procedure (1) can be interpreted as gradient descent applied to a quadratic regularized loss function and as a discrete dynamical system that spreads the initial value condition $F^{(0)} = Y$ through the graph via a linear gradient flow. We briefly review these two analogous formulations. Let ψ be the quadratic energy loss function that is separable on the columns of F :

$$\psi(F) = \sum_{\ell=1}^c \psi_{\ell}(F_{:, \ell}) = \sum_{\ell=1}^c \frac{1}{2} \{ \|F_{:, \ell} - Y_{:, \ell}\|_2^2 + \lambda F_{:, \ell}^{\top} \Delta F_{:, \ell} \}, \quad (2)$$

where $\Delta = I - D_G^{-1/2} A D_G^{-1/2} = I - S$ is the normalized Laplacian. Consider the the dynamical system

$$\dot{f}(t) = -\nabla \psi_{\ell}(f(t)) \quad (3)$$

for any $\ell \in \{1, \dots, L\}$. Since ψ_ℓ is convex, $\lim_{t \rightarrow \infty} f(t) = f^*$ such that $\psi_\ell(f^*) = \min \psi_\ell(f)$. Label spreading coincides with gradient descent applied to (2) or, equivalently, with explicit Euler integration applied to (3), for a particular value of the step length h . In fact,

$$f - h\nabla\psi_\ell(f) = f - h(f - Y_{:, \ell} + \lambda\Delta f) = (1 - h - h\lambda)f + h\lambda Sf + hY_{:, \ell}, \quad (4)$$

which, for $(1 - h)/h = \lambda$, coincides with one iteration of (1) applied to the ℓ -th column of F . Moreover, as $F^{(r)} \geq 0$ for all r , this gradient flow interpretation shows that the global minimizer of (2) is nonnegative, i.e., $\min \psi(F) = \min\{\psi(F) : F \geq 0\}$. In the next section, we use similar techniques to derive our nonlinear higher-order label spreading method.

3 Nonlinear Higher-order Label Spreading

Now we develop our nonlinear higher-order label spreading (NHOLS) technique. We will assume that we have a 3-regular hypergraph $H = (V, \mathcal{E}, \tau)$ capturing higher-order information on the same set of nodes as a weighted graph $G = (V, E, \omega)$, where $\mathcal{E} \subseteq V \times V \times V$ and τ is a hyperedge weight function $\tau(ijk) > 0$. In our experiments, we will usually derive H from G by considering the hyperedges of H to be the set of triangles (i.e., 3-cliques) of G . However, in principle we could use any hypergraph. We also do not need the associated graph G , but we keep it for greater generality and find it useful in practice. Finally, we develop our methodology for 3-regular hypergraphs for simplicity and notational sanity, but our ideas generalize to arbitrary hypergraphs (Theorem 3.3).

3.1 Nonlinear Second-order Label Spreading with Mixing Functions

We represent H via the associated third-order adjacency tensor \mathcal{A} , defined by $\mathcal{A}_{ijk} = \tau(ijk)$ if $ijk \in \mathcal{E}$ and $\mathcal{A}_{ijk} = 0$ otherwise. Analogous to the graph case, let $D_H = \text{Diag}(\delta_1, \dots, \delta_n)$ be the diagonal matrix of the hypergraph node degrees, where $\delta_i = \sum_{j,k: ijk \in \mathcal{E}} \tau(ijk) = \sum_{jk} \mathcal{A}_{ijk}$. Again, we assume that H has no isolated nodes so that $\delta_i > 0$ for all $i \in V$.

As noted in the introduction, we will make use of nonlinear *mixing functions*, which we denote by $\sigma: \mathbb{R}^2 \rightarrow \mathbb{R}$. For a tensor $T = T_{ijk}$, we define the tensor map $T\sigma: \mathbb{R}^n \rightarrow \mathbb{R}^n$ entrywise:

$$T\sigma(f)_i = \sum_{jk} T_{ijk} \sigma(f_j, f_k). \quad (5)$$

Hence, in analogy with the matrix case, we denote by $\mathcal{S}: \mathbb{R}^n \rightarrow \mathbb{R}^n$ the map

$$\mathcal{S}(f) = D_H^{-1/2} \mathcal{A}\sigma(D_H^{-1/2} f)$$

This type of tensor contraction will serve as the basis for our NHOLS technique.

We need one additional piece of notation that is special to the higher-order case, which is a type of energy function that will be used to normalize iterates in order to guarantee convergence. Let B be the matrix with entries $B_{ij} = \sum_k \mathcal{A}_{kij}$. Define $\varphi: \mathbb{R}^n \rightarrow \mathbb{R}$ by

$$\varphi(f) = \frac{1}{2} \sqrt{\sum_{ij} B_{ij} \sigma(f_i/\sqrt{\delta_i}, f_j/\sqrt{\delta_j})^2}. \quad (6)$$

Finally, we arrive at our nonlinear higher-order label spreading (NHOLS) method. Given an initial vector $f^{(0)} \in \mathbb{R}^n$, we define the NHOLS iterates by

$$g^{(r)} = \alpha \mathcal{S}(f^{(r)}) + \beta S f^{(r)} + \gamma y, \quad f^{(r+1)} = g^{(r)} / \varphi(g^{(r)}), \quad r = 0, 1, 2, \dots, \quad (7)$$

where $\alpha, \beta, \gamma \geq 0$, $\alpha + \beta + \gamma = 1$, and y is an initial label membership vector. Provided that σ is positive (i.e., $\sigma(a, b) > 0$ for any $a, b > 0$) and the initial vector $f^{(0)}$ is nonnegative, then all iterates are nonnegative. This assumption on the mixing function will be crucial to prove the convergence of the iterates. We perform this iteration with one initial vector per label class, analogous to standard Label Spreading. Algorithm 1 gives the overall procedure.

The parameters α, β, γ allow us to tune the contributes of the first-order local consistency, second-order local consistency, and global consistency. For $\beta = 0$ we obtain a purely second-order method, which can be useful when we do not have access to first-order data (e.g., we only have a hypergraph). The case of $\alpha = 0$ reduces to a normalized version of the standard LS as in (1). Furthermore, we can compute the iteration in (7) efficiently. Each iteration requires one matrix-vector product and one ‘‘tensor-matrix’’ product, which only takes a single pass over

Algorithm 1: NHOLS: Nonlinear Higher-Order Label Spreading

Input: Tensor \mathcal{A} ; matrix A ; mixing function $\sigma : \mathbb{R}^2 \rightarrow \mathbb{R}$; label matrix $Y \in \{0, 1\}^{n \times c}$; scalars $\alpha, \beta, \gamma \geq 0$ with $\alpha + \beta + \gamma = 1$; smoothing parameter $0 < \varepsilon < 1$; stopping tolerance tol

Output: Predicted labels $\hat{Y} \in \{1, \dots, c\}^n$

```
1  $\tilde{F} \in \mathbb{R}^{n \times c}$  # Store approximate solutions
2 for  $\ell = 1, \dots, L$  do
3    $y_\varepsilon \leftarrow (1 - \varepsilon)Y_{:, \ell} + \varepsilon \mathbf{1}$ 
4    $f^{(0)} \leftarrow y_\varepsilon$  # Initialize with label smoothing
5   repeat
6      $g \leftarrow \alpha \mathcal{S}(f^{(r)}) + \beta S f^{(r)} + \gamma y_\varepsilon$  # Following (5) and (7)
7      $f^{(r+1)} \leftarrow g / \varphi(g)$  # Following (6) and (7)
8   until  $\|f^{(r+1)} - f^{(r)}\| / \|f^{(r+1)}\| < \text{tol}$ 
9    $\tilde{F}_{:, \ell} \leftarrow f^{(r+1)}$ 
10 end
11 for  $i = 1, \dots, n$  do  $\hat{Y}_i = \arg \max_\ell \tilde{F}_{i, \ell}$ 
```

the input data with computational cost linear in the size of the data. Finally, Algorithm 1 uses label smoothing in the initialization (the parameter ε). This will be useful for proving convergence results and can also improve generalization [41].

The special case of a linear mixing function. The mixing function σ is responsible for the nonlinearity of the method. The linear mixing function $\sigma(a, b) = a + b$ reduces NHOLS to a clique-expansion approach, which corresponds to a normalized version of [60] for $\beta = 0$. To see this, let K be the $n \times |\mathcal{E}|$ incidence matrix of the hypergraph H , where $K_{i,e} = 1$ if node i is in the hyperedge e and $K_{i,e} = 0$ otherwise; furthermore, let W be the diagonal matrix of hyperedge weights $\tau(e)$, $e \in \mathcal{E}$. Then $2(KWK^\top)_{ij} = \sum_k \mathcal{A}_{ijk} + \mathcal{A}_{ikj}$. Thus, for $\sigma(a, b) = a + b$,

$$\mathcal{S}(f)_i = \delta_i^{-1/2} \sum_{jk} \mathcal{A}_{ijk} \delta_j^{-1/2} f_j + \mathcal{A}_{ijk} \delta_k^{-1/2} f_k = \delta_j^{-1/2} \sum_j \left(\sum_k \mathcal{A}_{ijk} + \mathcal{A}_{ikj} \right) \delta_j^{-1/2} f_j = (\Theta f)_i, \quad (8)$$

where $\Theta = 2D_H^{-1/2} KWK^\top D_H^{-1/2}$ is the normalized adjacency of the clique expansion graph [60].

3.2 Global convergence and optimization framework

Our NHOLS method extends standard LS in a natural way. However, with the nonlinear mixing function σ , it is unclear if the iterates even converge or to what they might converge. In this section, we show that, remarkably, NHOLS is globally convergent for a broad class of mixing functions and is minimizing a regularized objective similar to (2). Lemmas used in the proofs are provided in Appendix A.

For convergence, we only require the mixing function to be positive and one-homogeneous. We recall below these two properties for a general map Φ :

$$\text{Positivity: } \Phi(x) > 0 \text{ for all } x > 0. \quad (9)$$

$$\text{One-homogeneity: } \Phi(c \cdot x) = c \cdot \Phi(x) \text{ for all coefficients } c > 0 \text{ and all } x. \quad (10)$$

For technical reasons, we require entry-wise positive initialization. This is the reason for the smoothed membership vectors $y_\varepsilon = (1 - \varepsilon)Y_{:, \ell} + \varepsilon \mathbf{1}$ in Algorithm 1. This assumption is not restrictive in practice as ε can be chosen fairly small, and we can also interpret this as a type of label smoothing [41, 48].

The following theorem says that the NHOLS iterates converge for a broad class of mixing functions. This is a corollary of a more general result that we prove later (Theorem 3.3).

Theorem 3.1. *Let $f^{(r)}$ be the iterates in Algorithm 1. If σ is positive and one-homogeneous, then the sequence $\{f^{(r)}\}_r$ converges to a unique stationary point $f^* > 0$ with $\varphi(f^*) = 1$.*

Even if the iterates converge, we would still like to know to what they converge. We next show that for differentiable mixing functions σ , a scaled version of f^* minimizes a regularized objective that enforces local and global consistency. For a smoothed membership vector $y_\varepsilon = (1 - \varepsilon)Y_{:, \ell} + \varepsilon \mathbf{1}$ with $0 < \varepsilon < 1$, consider the loss function:

$$\vartheta(f) = \frac{1}{2} \left\{ \left\| f - \frac{y_\varepsilon}{\varphi(y_\varepsilon)} \right\|_2^2 + \lambda \sum_{ij} \mathcal{A}_{ij} \left(\frac{f_i}{\sqrt{d_i}} - \frac{f_j}{\sqrt{d_j}} \right)^2 + \mu \sum_{ijk} \mathcal{A}_{ijk} \left(\frac{f_i}{\sqrt{d_i}} - \frac{1}{2} \sigma \left(\frac{f_j}{\sqrt{d_j}}, \frac{f_k}{\sqrt{d_k}} \right) \right)^2 \right\} \quad (11)$$

As for the case of standard LS, ϑ consists of a global consistency term regularized by a local consistency term. However, there are two main differences. First, the global consistency term now considers a normalized membership vector $\tilde{y}_\varepsilon = y_\varepsilon/\varphi(y_\varepsilon)$. As $\varphi(\tilde{y}_\varepsilon) = 1$, we seek for a minimizer of ϑ in the slice $\{f : \varphi(f) = 1\}$. Second, the regularizer now combines the normalized Laplacian term with a new tensor-based term that accounts for higher-order interactions.

Analogous to standard LS, NHOLS can be interpreted as a projected diffusion process that spreads the input label assignment via the nonlinear gradient flow corresponding to the energy function $\tilde{\vartheta}(f) = \vartheta(f) - \frac{\mu}{2}\varphi(f)^2$. In fact, for y_ε such that $\varphi(y_\varepsilon) = 1$, we have that

$$f - h\nabla\tilde{\vartheta}(f) = (1 - h - \lambda h + \mu h)f + h\lambda Sf + h\mu\mathcal{S}(f) + hy_\varepsilon. \quad (12)$$

(A proof of this identity is the proof of Theorem 3.2.) Thus, our NHOLS iterates in (7) correspond to projected gradient descent applied to $\tilde{\vartheta}$, with step length h chosen so that $(1 - h)/h = \lambda + \mu$. This is particularly useful in view of (11), since $\tilde{\vartheta}$ and ϑ have the same minimizing points on $\{f : \varphi(f) = 1\}$. Moreover, as $\nabla\psi$ in (3) can be interpreted as a discrete Laplacian operator on the graph [59], we can interpret $\nabla\tilde{\vartheta}$, and thus \mathcal{S} , as a hypergraph Laplacian operator, which adds up to the recent literature on (nonlinear) Laplacians on hypergraphs [12, 38].

Unlike the standard label spreading, the loss functions ϑ and $\tilde{\vartheta}$ are not convex in general. Thus, the long-term behavior $\lim_{t \rightarrow \infty} f(t)$ of the gradient flow $\dot{f}(t) = -\nabla\tilde{\vartheta}(f(t))$ is not straightforward. Despite this, the next Theorem 3.2 shows that the NHOLS can converge to a unique global minimizer of ϑ over the set of nonnegative vectors. For this result, we need an additional assumption of differentiability on the mixing function σ .

Theorem 3.2. *Let $f^{(r)}$ be the sequence generated by Algorithm 1. If σ is positive, one-homogeneous, and differentiable, then the sequence $\{f^{(r)}\}_r$ converges to the unique global solution of the constrained optimization problem*

$$\min \vartheta(f) \text{ s.t. } f > 0 \text{ and } \varphi(f) = 1. \quad (13)$$

Proof. Let

$$E_1(f) = \sum_{ij} A_{ij}(f_i/\sqrt{d_i} - f_j/\sqrt{d_j})^2, \quad E_2(f) = \sum_{ijk} \mathcal{A}_{ijk}(f_i/\sqrt{d_i} - \sigma(f_j/\sqrt{d_j}, f_k/\sqrt{d_k})/2)^2$$

and consider the following modified loss

$$\tilde{\vartheta}(f) = \frac{1}{2} \left\{ \left\| f - \frac{y}{\varphi(y)} \right\|^2 + \lambda E_1(f) + \mu E_2(f) - \mu \varphi(f)^2 \right\},$$

Clearly, when subject to $\varphi(f) = 1$, the minimizing points of $\tilde{\vartheta}$ and those of ϑ in (11) coincide. We show that the gradient of the loss function $\tilde{\vartheta}$ vanishes on $f^* > 0$ with $\varphi(f^*) = 1$ if and only if f^* is a fixed point for the iterator of Algorithm 1.

For simplicity, let us write $\tilde{y} = y/\varphi(y)$ with $y > 0$. We have $\nabla\|f - \tilde{y}\|^2 = 2(f - \tilde{y})$ and $\nabla E_1(f) = 2\Delta f = 2(I - D_G^{-1}AD_G^{-1})f$. As for E_2 , observe that from $\sum_{jk} \mathcal{A}_{ijk} = \delta_i$, we get

$$\begin{aligned} f^\top(D_H f - \mathcal{A}\sigma(f)) &= \sum_i \delta_i f_i^2 - \sum_{ijk} f_i \mathcal{A}_{ijk} \sigma(f_j, f_k) = \sum_{ijk} \mathcal{A}_{ijk} (f_i^2 - f_i \sigma(f_j, f_k)) \\ &= \sum_{ijk} \mathcal{A}_{ijk} \left(f_i - \frac{\sigma(f_j, f_k)}{2} \right)^2 - \frac{1}{4} \sum_{jk} B_{jk} \sigma(f_j, f_k)^2 \end{aligned}$$

with $B_{jk} = \sum_i \mathcal{A}_{ijk}$. Thus, it holds that

$$f^\top(D_H f - \mathcal{A}\sigma(f)) = E_2(D_H^{1/2} f) - \varphi(D_H^{1/2} f)^2.$$

Now, since $\sigma(f)$ is one-homogeneous and differentiable, so is $F(f) = \mathcal{P}\sigma(f)$, and using Lemma A.3 we obtain $\nabla\{E_2(D_H^{1/2} f) - \varphi(D_H^{1/2} f)^2\} = 2(D_H f - \mathcal{A}\sigma(f))$ which, with the change of variable $f \mapsto D_H^{-1/2} f$, yields

$$\nabla\{E_2(f) - \varphi(f)^2\} = f - D_H^{-1/2} \mathcal{A}\sigma(D_H^{-1/2} f)$$

Altogether we have that

$$\begin{aligned} \nabla\tilde{\vartheta}(f) &= f - \tilde{y} + \lambda(I - D_G^{-1/2}AD_G^{-1/2})f + \mu\{f - D_H^{-1/2} \mathcal{A}\sigma(D_H^{-1/2} f)\} \\ &= (1 + \lambda + \mu)f - \lambda D_G^{-1/2}AD_G^{-1/2}f - \mu D_H^{-1/2} \mathcal{A}\sigma(D_H^{-1/2} f) - \tilde{y}, \end{aligned}$$

which implies that $f^* \in \mathbb{R}_{++}^n / \varphi$ is such that $\nabla \tilde{\vartheta}(f^*) = 0$ if and only if f^* is a fixed point of NHOLS, i.e.

$$f^* = \alpha D_H^{-1/2} \mathcal{A} \sigma(D_H^{-1/2} f^*) + \beta D_G^{-1/2} A D_G^{-1/2} f^* + \gamma \tilde{y}$$

with $\lambda = \beta/\gamma$, $\mu = \alpha/\gamma$ and $\alpha + \beta + \gamma = 1$.

Finally, by Theorem 3.1 we know that the NHOLS iterations in Algorithm 1 converge to $f^* > 0$, $\varphi(f^*) = 1$ for all positive starting points $f^{(0)}$. Moreover, f^* is the unique fixed point in the slice $\mathbb{R}_{++}^n / \varphi = \{f > 0 : \varphi(f) = 1\}$. As ϑ and $\tilde{\vartheta}$ have the same minimizing points on that slice, this shows that f^* is the global solution of $\min\{\vartheta(f) : f \in \mathbb{R}_{++}^n / \varphi\}$, concluding the proof. \square

3.3 Main convergence result and extension to other orders

Theorem 3.1 is a direct consequence of our main convergence theorem below, where $F(f) = \alpha D_H^{-1/2} \mathcal{A} \sigma(D_H^{-1/2} f) + \beta D_G^{-1/2} A D_G^{-1/2} f$ and $y = \gamma y_\varepsilon$. By Lemma A.2 all of the assumptions for Theorem 3.3 are satisfied, and the convergence follows.

Theorem 3.3. *Let $F : \mathbb{R}^n \rightarrow \mathbb{R}^n$ and $\varphi : \mathbb{R}^n \rightarrow \mathbb{R}$ be positive and one-homogeneous mappings, and let y be a positive vector. If there exists $C > 0$ such that $F(f) \leq Cy$, for all f with $\varphi(f) = 1$, then, for any $f^{(0)} > 0$, the sequence*

$$g^{(r)} = F(f^{(r)}) + y \quad f^{(r+1)} = g^{(r)} / \varphi(g^{(r)})$$

converges to $f^* > 0$, unique fixed point of $F(f) + y$ such that $\varphi(f^*) = 1$.

This general convergence result makes it clear how to transfer the second-order setting discussed in this work to hyperedges of any order. For example, nonlinearities could be added to the graph term as well. A nonlinear purely first-order label spreading has the general form $f^{(r+1)} = \beta M \sigma(f^{(r)}) + \gamma y$, where $M \sigma(f)$ is the vector with entries $M \sigma(f)_i = \sum_j M_{ij} \sigma(f_j)$, σ is a nonlinear map and M is a graph matrix. This formulation is quite general and provides new convergence results for nonlinear graph diffusions recently proposed by Ibrahim and Gleich [26]. For simplicity and in the interest of space, we do not use this extension in our experiments, but out of theoretical interest we note that Theorem 3.3 would allow us to take this additional nonlinearity into account.

Proof. Let $\varphi : \mathbb{R}^n \rightarrow \mathbb{R}$ and $F : \mathbb{R}^n \rightarrow \mathbb{R}^n$ be one-homogeneous and positive maps. Let \mathbb{R}_+^n and \mathbb{R}_{++}^n denote the set of entrywise nonnegative and entrywise positive vectors in \mathbb{R}^n , respectively. Also, let $\mathbb{R}_{++}^n / \varphi = \{f \in \mathbb{R}_{++}^n : \varphi(f) = 1\}$. This result falls within the family of Denjoy-Wolff type theorems for nonlinear mappings on abstract cones, see e.g., Lemmens et al. [34]. Here we provide a simple and self-contained proof. Define

$$G(f) = F(f) + y \quad \text{and} \quad \tilde{G}(f) = \frac{G(f)}{\varphi(G(f))}.$$

Notice that $f^{(r+1)} = \tilde{G}(f^{(r)})$, $r = 0, 1, 2, \dots$ and that, by assumption, $G(f) > 0$ for all $f > 0$. Thus $\varphi(G(f)) > 0$ and $\tilde{G}(f)$ is well defined on \mathbb{R}_{++}^n . Moreover, \tilde{G} preserves the cone slice $\mathbb{R}_{++}^n / \varphi$ i.e. $\tilde{G}(f) \in \mathbb{R}_{++}^n / \varphi$ for all $f \in \mathbb{R}_{++}^n / \varphi$. For two points $u, v \in \mathbb{R}_{++}^n$ let

$$d(u, v) = \log \left(\frac{M(u/v)}{m(u/v)} \right)$$

be the Hilbert distance, where $M(u/v) = \max_i u_i / v_i$ and $m(u/v) = \min_i u_i / v_i$. As σ is one-homogeneous also φ is one-homogeneous and thus $\mathbb{R}_{++}^n / \varphi$ equipped with the Hilbert distance is a complete metric space, [20] e.g. In order to conclude the proof it is sufficient to show that \tilde{G} is a contraction with respect to such metric. In fact, the sequence $f^{(r)}$ belongs to $\mathbb{R}_{++}^n / \varphi$ for any $f^{(0)}$ and since $(\mathbb{R}_{++}^n / \varphi, d)$ is complete, the sequence $f^{(r)}$ converges to the unique fixed point f^* of \tilde{G} in $\mathbb{R}_{++}^n / \varphi$.

We show below that \tilde{G} is a contraction. To this end, first note that by definition we have $d(\tilde{G}(u), \tilde{G}(v)) = d(G(u), G(v))$. Now note that, as σ is homogeneous and order preserving, for any $u, v \in \mathbb{R}_{++}^n$ we have $m(u/v)F(v) = F(m(u/v)v) \leq F(u)$, $M(u/v)F(v) = F(M(u/v)v) \geq F(u)$, $m(u/v)\varphi(v) = \varphi(m(u/v)v) \leq \varphi(u)$ and $M(u/v)\varphi(v) = \varphi(M(u/v)v) \geq \varphi(u)$. Moreover, for any $u, v \in \mathbb{R}_{++}^n / \varphi$ it holds

$$m(u/v) = \varphi(u)m(u/v) \leq \varphi(v) = 1 \leq \varphi(u)M(u/v) = M(u/v),$$

thus $m(u/v) \leq 1 \leq M(u/v)$. By assumption there exists $C > 0$ such that $F(u) \leq Cy$, for all $u \in \mathbb{R}_{++}^n/\varphi$. Therefore, for any $u, v \in \mathbb{R}_{++}^n/\varphi$, we have

$$\begin{aligned} (m(u/v)C + 1)(F(v) + y) &= (m(u/v)C + m(u/v) - m(u/v) + 1)F(v) + (m(u/v)C + 1)y \\ &= m(u/v)CF(v) + m(u/v)F(v) + (1 - m(u/v))F(v) + (m(u/v)C + 1)y \\ &\leq CF(u) + F(u) + (1 - m(u/v))Cy + (m(u/v)C + 1)y \\ &= (C + 1)(F(u) + y) \end{aligned}$$

where we used the fact that $(1 - m(u/v)) \geq 0$ to get $(1 - m(u/v))F(v) \leq (1 - m(u/v))Cy$. Thus

$$m(G(u)/G(v)) = m((F(u) + y)/(F(v) + y)) \geq (m(u/v)C + 1)/(C + 1).$$

Similarly, as $(1 - M(u/v)) \leq 0$, we have

$$\begin{aligned} (M(u/v)C + 1)(F(v) + y) &\geq CF(u) + F(u) + (1 - M(u/v))Cy + (M(u/v)C + 1)y \\ &= (C + 1)(F(u) + y) \end{aligned}$$

which gives $M(G(u)/G(v)) \leq (M(u/v)C + 1)/(C + 1)$. Therefore,

$$d(G(u), G(v)) = \log \left(\frac{M(G(u)/G(v))}{m(G(u)/G(v))} \right) \leq \log \left(\frac{M(u/v)C + 1}{m(u/v)C + 1} \right) = \log \left(\frac{M(u/v) + \delta}{m(u/v) + \delta} \right)$$

with $\delta = 1/C$. Finally, using Lemma A.1 we get

$$d(\tilde{G}(u), \tilde{G}(v)) = d(G(u), G(v)) \leq \left(\frac{M(u/v)}{M(u/v) + \delta} \right) d(u, v) < d(u, v)$$

which shows that \tilde{G} is a contraction in the complete metric space $(\mathbb{R}_{++}^n/\varphi, d)$. \square

4 Experiments

We now perform experiments on both synthetic and real-world data. Our aim is to compare the performance of standard (first-order) label spreading algorithm with our second-order methods, using different mixing functions σ . Based on (11), a natural class of functions are the one-parameter family of generalized p -means scaled by factor 2, i.e., $\sigma_p(a, b) = 2((a^p + b^p)/2)^{1/p}$. In particular, we consider the following generalized means:

name	arithmetic	harmonic	L^2	geometric	maximum
p	$p = 1$	$p = -1$	$p = 2$	$p \rightarrow 0$	$p \rightarrow \infty$
$\sigma_p(a, b)$	$(a + b)$	$4(\frac{1}{a} + \frac{1}{b})^{-1}$	$2\sqrt{\frac{a^2 + b^2}{2}}$	$2\sqrt{ab}$	$2 \cdot \max(a, b)$

The function σ_p is one-homogeneous, positive, and order-preserving for all values of $p \in \mathbb{R}$, including the limit cases of $p \in \{0, +\infty\}$. Thus, by Theorem 3.1, Algorithm 1 converges for any choice of p . The maximum function, however, is not differentiable and thus we cannot prove the computed limit of the sequence $f^{(r)}$ optimizes the loss function (11) (but one can approximate the maximum with a large finite p , and use Theorem 3.2 on such smoothed max). Also, as shown above, the case $p = 1$ (i.e., σ_p linear) essentially corresponds to a clique expansion method, so Algorithm 1 is nearly the same as the local and global consistency method for semi-supervised learning [59], where the adjacency matrix is a convex combination of the clique expansion graph induced by the tensor \mathcal{A} and the graph A . In our experiments, we use at most 40 iterations within Algorithm 1, a stopping tolerance of $1e-5$, and smoothing parameter $\varepsilon = 0.01$. Other tolerances and other ε gave similar results. The code for implementing NHOLS is available at <https://github.com/doublelucker/nhols>.

In addition to comparing against standard label spreading, we also compare against two other techniques. The first is hypergraph total variation (HTV) minimization, which is designed for clustering hypergraphs with larger hyperedges but is still applicable to our setup [24]. This is a state-of-the-art method for pure hypergraph data. The second is a graph neural network (GNN) approach, which is broadly considered state-of-the-art for first-order methods. More specifically, we use GraphSAGE [23] with two layers, ReLU activation, and mean aggregation, using node features if available and one-hot encoding features otherwise. Neither of these baselines incorporate both first- and second-order information in the graph, as NHOLS.

All of the algorithms that we use have hyperparameters. For the label spreading and HTV methods, we run 5-fold cross validation with label-balanced 50/50 splits over a small grid to choose these hyperparameters. For standard label

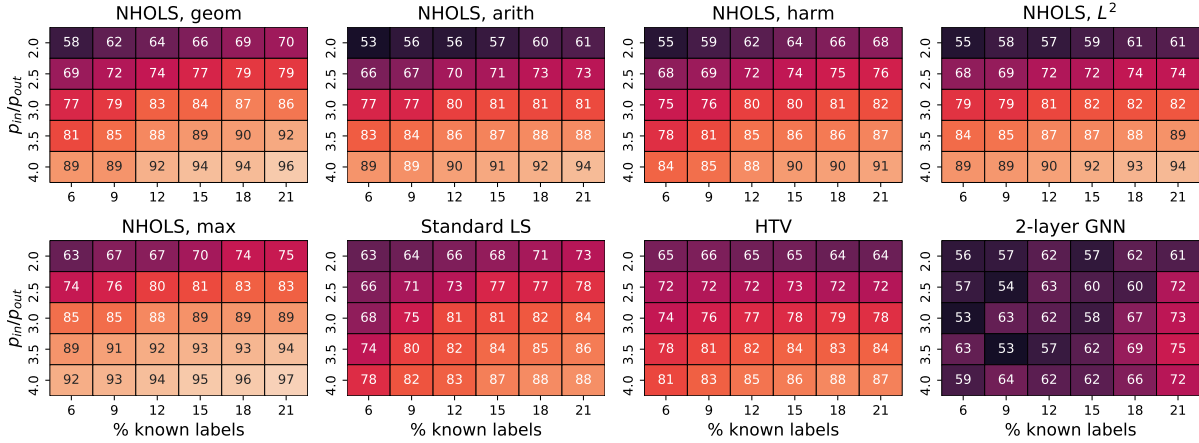


Figure 1: Accuracy on synthetic stochastic block models. Each table corresponds to a different method, and table entries are the average accuracy over 10 random instances with the given parameter settings. Overall, the various NHOLS methods perform much better than the baselines.

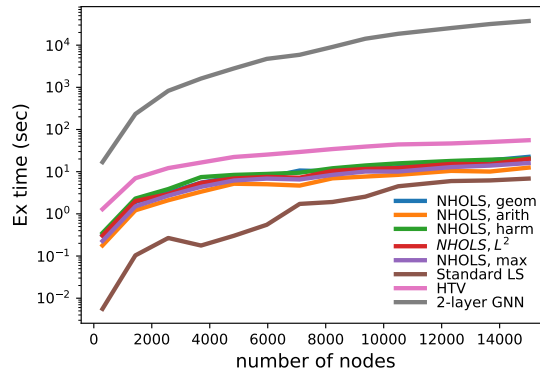


Figure 2: Running times of various algorithms for a single hyperparameter setting with SBM data. NHOLS scales linearly with the number of nonzeros in \mathcal{S} and \mathcal{S} and costs a little more than standard LS. HTV is a bit little slower, and the GNN is several orders of magnitude slower for even modest network sizes.

spreading, the grid is $\beta \in \{0.1, 0.2, \dots, 0.9\}$. For higher-order label spreadings, the grid is $\alpha \in \{0.3, 0.4, \dots, 0.8\}$ and $\beta \in \{0.1, 0.25, 0.40, 0.55\}$ (subject to the constraint that $\alpha + \beta < 1$). HTV has a regularization term λ , which we search over $\lambda = (1 - \beta)/\beta$ for $\beta \in \{0.1, 0.2, \dots, 0.9\}$ (i.e., the same grid as LS). We choose the parameters that give the best average accuracy over the five folds. The GNN is much slower, so we split the labeled data into a training and validation sets with a label-balanced 50/50 split (i.e., a 1-fold cross validation, as is standard for training such models). We use ADAM optimizer with default β parameters and search over learning rates $\eta \in \{0.01, 0.001, 0.0001\}$ and weight decays $\omega \in \{0, 0.0001\}$, using 15 epochs.

4.1 Synthetic benchmark data

s We first compare the semi-supervised learning algorithms on synthetic graph data generated with the Stochastic Block Model (SBM). The SBM is a generative model for graph data with prescribed cluster structure. We use the variant of an SBM with two parameters — p_{in} and p_{out} — which designate the edge probabilities within the same label and across different labels, respectively. Generative block models are a common benchmark to test the performance of semi-supervised learning methods [29, 31, 39, 40]. Here we analyze the performance of different methods on random graphs drawn from the SBM where nodes belong to three different classes of size (number of nodes) 100, 200 and 400. We sample graphs for different values of the parameters p_{in} and p_{out} ; precisely, we fix $p_{\text{in}} = 0.1$ and let $p_{\text{out}} = p_{\text{in}}/\rho$ for $\rho \in \{2, 2.5, 3, 3.5, 4\}$. We test the various algorithms for different percentages of known labels per each class ($\{6\%, 9\%, 12\%, 15\%, 18\%, 21\%\}$). With this setting, small values of ρ correspond to more difficult classification problems.

Table 1: Mean accuracy over five random samples of labeled nodes over six datasets and four percentages of labeled nodes. We compare our NHOLS method using five different mixing functions to standard LS, Hypergraph Total Variation minimization [24] and a Graph Neural Network model [23]. Incorporating higher-order information into label spreading always improves performance. HTV is sometimes competitive, and the GNN has poor performance.

method	% labeled	Rice31 (n = 3560)				Caltech36 (n = 590)			
		5.0%	10.0%	15.0%	20.0%	5.0%	10.0%	15.0%	20.0%
NHOLS, arith		88.0	89.7	90.8	91.1	80.9	82.0	85.3	85.4
NHOLS, harm		88.1	89.6	90.7	91.3	79.6	81.7	84.6	84.9
NHOLS, L^2		88.0	89.7	90.7	91.2	80.7	82.3	85.0	85.3
NHOLS, geom		87.9	89.7	90.7	91.2	80.3	82.3	84.8	85.0
NHOLS, max		87.6	89.3	90.3	90.7	81.0	82.3	86.0	85.3
Standard LS		83.1	87.6	89.5	90.6	70.1	76.6	80.9	81.9
HTV		81.6	85.7	87.7	90.0	66.1	76.1	75.9	81.8
2-layer GNN		54.2	69.2	79.1	80.6	44.6	44.3	61.6	54.2
method	% labeled	optdigits (n = 5620)				pendigits (n = 10992)			
		0.4%	0.7%	1.0%	1.3%	0.4%	0.7%	1.0%	1.3%
NHOLS, arith		94.9	95.7	96.2	97.5	91.1	91.4	95.4	95.8
NHOLS, harm		93.2	95.5	95.8	97.2	90.7	91.2	95.4	95.6
NHOLS, L^2		95.5	95.7	96.3	97.7	91.1	91.5	95.4	95.7
NHOLS, geom		94.0	95.6	95.9	97.4	91.0	91.3	95.4	95.7
NHOLS, max		94.8	95.8	95.9	97.4	93.6	92.8	95.9	95.9
Standard LS		93.8	93.8	95.6	96.7	91.3	92.0	95.3	95.0
HTV		87.0	90.9	93.3	94.1	82.2	91.3	93.3	93.3
2-layer GNN		52.1	62.6	70.9	73.6	56.8	67.7	63.0	64.4
method	% labeled	MNIST (n = 60000)				Fashion-MNIST (n = 60000)			
		0.1%	0.3%	0.5%	0.7%	0.1%	0.3%	0.5%	0.7%
NHOLS, arith		92.6	95.3	95.7	95.9	71.0	75.6	77.9	78.2
NHOLS, harm		91.8	94.9	95.6	95.8	70.8	75.3	77.9	78.1
NHOLS, L^2		92.7	95.4	95.8	95.9	71.3	75.6	77.7	78.3
NHOLS, geom		92.0	95.0	95.6	95.8	70.6	75.3	77.8	77.9
NHOLS, max		92.3	95.3	95.7	95.8	69.7	75.4	77.0	77.9
Standard LS		87.6	92.2	93.6	94.1	68.6	73.4	76.5	77.4
HTV		79.7	88.3	90.1	90.7	59.8	68.6	70.2	72.0
2-layer GNN		60.5	77.5	81.5	84.9	63.2	71.8	73.0	73.7

The colored tables in Figure 1 show the average clustering accuracy over ten random samples for each SBM setting and each percentage of input labels. We observe that the nonlinear label spreading methods perform best overall, with the maximum function performing the best in nearly all the cases. The performance gaps can be quite substantial. For example, when only 6% of the labels are given, NHOLS achieves up to 92% mean accuracy, while the baselines do not achieve greater than 81%.

Moreover, NHOLS scales linearly with the number of nonzero elements of \mathcal{S} and S and thus is typically just slightly more expensive than standard LS. This is illustrated in Figure 2, where we compare mean execution time over ten runs for different methods. We generate random SBM graphs with three labels of equal size, increasing number of nodes n and edge probabilities $p_{in} = \log(n)^2/n$ and $p_{out} = p_{in}/3$. Each method is run with a fixed value of the corresponding hyperparameters, chosen at random each time. We note that HTV and GNN are around one and three-to-five orders of magnitude slower than NHOLS, respectively.

4.2 Real-world data

We also analyze the performance of our methods on six real-world datasets (Table 1). The first two datasets come from relational networks, namely Facebook friendship graphs of Rice University and Caltech from the Facebook100 collection [49]. The labels are the dorms in which the students live — there are 9 dorms for Rice and 8 for Caltech. Facebook friendships form edges, and the tensor entries correspond to triangles (3-cliques) in the graph. We preprocessed the graph data by first removing students with missing labels and then taking the largest connected component of the resulting graph. The GNN uses a one-hot encoding for features.

The next four graphs are derived from point clouds: optdigits [15, 55], pendigits [4, 15], MNIST [33], and Fashion-MNIST [54]. Each of these datasets has 10 classes, corresponding to one of 10 digits or to one of 10 fashion items. In these cases, we first create 7-nearest-neighbor graphs. Tensor entries correspond to triangles in this graph. We give the GNN an additional advantage by providing node features derived from the data points. The optdigits and pendigits datasets come with several hand-crafted features; and we use the embedding in first 10 principal components for node features. The MNIST and Fashion-MNIST datasets contain the raw images; here, we use an embedding from the first 20 principal components of the images as node features for the GNN. (We also tried one-hot encodings and the raw data points as features, both of which had much worse performance.)

We recorded the mean accuracy of five random samples of labeled nodes (Table 1). We find that incorporating higher-order information with some mixing function improves performance of LS in nearly all cases and also outperforms the baselines. The absolute accuracy of these methods is also quite remarkable; for example, the L^2 mixing function achieves 92.7% mean accuracy with just 0.1% of MNIST points labeled (6 samples per class) and the maximum mixing function achieves 93.6% mean accuracy with just 0.4% of pendigits points labeled (5 samples per class). Also, a single mixing function tends to have the best performance on a given dataset, regardless of the number of available labels (e.g., the maximum mixing function for Caltech36 and pendigits, the L^2 mixing function for MNIST and Fashion-MNIST).

Finally, the GNN performance is often poor, even in cases where meaningful node features are available. This is likely a result of having only a small percentage of labeled examples. For example, it is common to have over 15% of the nodes labeled just as a validation set for hyperparameter tuning [30]. Still, even with 20% of nodes labeled and hyperparameter tuning, the GNN performs much worse than all other methods on the Facebook graphs.

5 Discussion

We have developed a natural and substantial extension of traditional label spreading for semi-supervised learning that can incorporate a broad range of nonlinearities into the spreading process. These nonlinearities come from mixing functions that operate on higher-order information associated with the data. Given the challenges in developing optimization results involving nonlinear functions, it is remarkable that we can achieve a sound theoretical framework for our expressive spreading process. We provided guarantees on convergence of the iterations to a unique solution, and we showed that the process optimizes a meaningful objective function. Finally, the convergence result in Theorem 3.3 is more general than what we considered in our experiments. This provides a new way to analyze nonlinearities in graph-based methods that we expect will be useful for future research.

Acknowledgments

We thank Matthias Hein for supplying the code that implements the HTV algorithm in [24]. We thank David Gleich and Antoine Gautier for helpful discussions. ARB is supported by NSF Award DMS-1830274, ARO Award W911NF19-1-0057, ARO MURI, and JPMorgan Chase & Co. FT is partially supported by INdAM-GNCS.

This research was funded in part by JPMorgan Chase & Co. Any views or opinions expressed herein are solely those of the authors listed, and may differ from the views and opinions expressed by JPMorgan Chase & Co. or its affiliates. This material is not a product of the Research Department of J.P. Morgan Securities LLC. This material should not be construed as an individual recommendation for any particular client and is not intended as a recommendation of particular securities, financial instruments or strategies for a particular client. This material does not constitute a solicitation or offer in any jurisdiction.

References

- [1] Sameer Agarwal, Kristin Branson, and Serge Belongie. Higher order learning with graphs. In *Proceedings of the 23rd international conference on Machine learning*, pages 17–24, 2006.
- [2] Nesreen K Ahmed, Jennifer Neville, Ryan A Rossi, Nick G Duffield, and Theodore L Willke. Graphlet decomposition: Framework, algorithms, and applications. *Knowledge and Information Systems*, 50(3):689–722, 2017.
- [3] Morteza Alamgir and Ulrike V Luxburg. Phase transition in the family of p-resistances. In *Advances in Neural Information Processing Systems*, pages 379–387, 2011.
- [4] Fevzi Alimoglu and Ethem Alpaydin. Methods of combining multiple classifiers based on different representations for pen-based handwritten digit recognition. In *Proceedings of the Fifth Turkish Artificial Intelligence and Artificial Neural Networks Symposium*. Citeseer, 1996.

- [5] Animashree Anandkumar, Rong Ge, Daniel Hsu, Sham M Kakade, and Matus Telgarsky. Tensor decompositions for learning latent variable models. *Journal of Machine Learning Research*, 15:2773–2832, 2014.
- [6] Francesca Arrigo, Desmond J Higham, and Francesco Tudisco. A framework for second-order eigenvector centralities and clustering coefficients. *Proceedings of the Royal Society A*, 476(2236):20190724, 2020.
- [7] Francesca Arrigo and Francesco Tudisco. Multi-dimensional, multilayer, nonlinear and dynamic hits. In *Proceedings of the 2019 SIAM International Conference on Data Mining*, pages 369–377. SIAM, 2019.
- [8] Austin R Benson. Three hypergraph eigenvector centralities. *SIAM Journal on Mathematics of Data Science*, 1(2):293–312, 2019.
- [9] Austin R Benson, Rediet Abebe, Michael T Schaub, Ali Jadbabaie, and Jon Kleinberg. Simplicial closure and higher-order link prediction. *Proceedings of the National Academy of Sciences*, 115(48):E11221–E11230, 2018.
- [10] Austin R Benson, David F Gleich, and Jure Leskovec. Higher-order organization of complex networks. *Science*, 353(6295):163–166, 2016.
- [11] Nick Bridle and Xiaojin Zhu. p-voltages: Laplacian regularization for semi-supervised learning on high-dimensional data. In *Eleventh Workshop on Mining and Learning with Graphs (MLG2013)*. Citeseer, 2013.
- [12] T-H Hubert Chan, Anand Louis, Zhihao Gavin Tang, and Chenzi Zhang. Spectral properties of hypergraph laplacian and approximation algorithms. *Journal of the ACM (JACM)*, 65(3):1–48, 2018.
- [13] Alex Chin, Yatong Chen, Kristen M. Altenburger, and Johan Ugander. Decoupled smoothing on graphs. In *The World Wide Web Conference*, pages 263–272, 2019.
- [14] Uthsav Chitra and Benjamin Raphael. Random walks on hypergraphs with edge-dependent vertex weights. In *International Conference on Machine Learning*, pages 1172–1181, 2019.
- [15] Dheeru Dua and Casey Graff. UCI machine learning repository, 2017.
- [16] Dhivya Eswaran, Srijan Kumar, and Christos Faloutsos. Higher-order label homogeneity and spreading in graphs. In *Proceedings of The Web Conference 2020*, pages 2493–2499, 2020.
- [17] Yifan Feng, Haoxuan You, Zizhao Zhang, Rongrong Ji, and Yue Gao. Hypergraph neural networks. In *Proceedings of the AAAI Conference on Artificial Intelligence*, volume 33, pages 3558–3565, 2019.
- [18] Yasuhiro Fujiwara and Go Irie. Efficient label propagation. In *International Conference on Machine Learning*, pages 784–792, 2014.
- [19] Antoine Gautier and Francesco Tudisco. The contractivity of cone-preserving multilinear mappings. *Nonlinearity*, 32:4713, 2019.
- [20] Antoine Gautier, Francesco Tudisco, and Matthias Hein. The Perron-Frobenius theorem for multihomogeneous mappings. *SIAM Journal on Matrix Analysis and Applications*, 40(3):1179–1205, 2019.
- [21] David F Gleich and Michael W Mahoney. Using local spectral methods to robustify graph-based learning algorithms. In *Proceedings of the 21th ACM SIGKDD International Conference on Knowledge Discovery and Data Mining*, pages 359–368, 2015.
- [22] Ian Goodfellow, Yoshua Bengio, and Aaron Courville. *Deep Learning*. MIT Press, 2016. <http://www.deeplearningbook.org>.
- [23] Will Hamilton, Zhitao Ying, and Jure Leskovec. Inductive representation learning on large graphs. In *Advances in neural information processing systems*, pages 1024–1034, 2017.
- [24] Matthias Hein, Simon Setzer, Leonardo Jost, and Syama Sundar Rangapuram. The total variation on hypergraphs - learning on hypergraphs revisited. In *Advances in Neural Information Processing Systems*, pages 2427–2435, 2013.
- [25] Thomas Hofmann, Bernhard Schölkopf, and Alexander J Smola. Kernel methods in machine learning. *The annals of statistics*, pages 1171–1220, 2008.
- [26] Rania Ibrahim and David Gleich. Nonlinear diffusion for community detection and semi-supervised learning. In *The World Wide Web Conference*, pages 739–750, 2019.
- [27] Ariel Jaffe, Roi Weiss, Boaz Nadler, Shai Carmi, and Yuval Kluger. Learning binary latent variable models: A tensor eigenpair approach. In *International Conference on Machine Learning*, pages 2196–2205, 2018.
- [28] Thorsten Joachims. Transductive learning via spectral graph partitioning. In *Proceedings of the 20th International Conference on Machine Learning (ICML-03)*, pages 290–297, 2003.
- [29] Varun Kanade, Elchanan Mossel, and Tselil Schramm. Global and local information in clustering labeled block models. *IEEE Transactions on Information Theory*, 62(10):5906–5917, 2016.

- [30] Thomas N. Kipf and Max Welling. Semi-supervised classification with graph convolutional networks. In *ICLR*, 2017.
- [31] Isabel M Kloumann, Johan Ugander, and Jon Kleinberg. Block models and personalized pagerank. *Proceedings of the National Academy of Sciences*, 114(1):33–38, 2017.
- [32] Rasmus Kyng, Anup Rao, Sushant Sachdeva, and Daniel A Spielman. Algorithms for lipschitz learning on graphs. In *Conference on Learning Theory*, pages 1190–1223, 2015.
- [33] Yann LeCun, Corinna Cortes, and CJ Burges. Mnist handwritten digit database, 2010.
- [34] Bas Lemmens, Brian Lins, Roger Nussbaum, and Marten Wortel. Denjoy-Wolff theorems for Hilbert’s and Thompson’s metric spaces. *Journal d’Analyse Mathématique*, 134(2):671–718, 2018.
- [35] Pan Li, I Chien, and Olgica Milenkovic. Optimizing generalized pagerank methods for seed-expansion community detection. In *Advances in Neural Information Processing Systems*, pages 11705–11716, 2019.
- [36] Pan Li and Olgica Milenkovic. Inhomogeneous hypergraph clustering with applications. In *Advances in Neural Information Processing Systems*, pages 2308–2318, 2017.
- [37] Pan Li and Olgica Milenkovic. Submodular hypergraphs: p-laplacians, cheeger inequalities and spectral clustering. In *International Conference on Machine Learning*, pages 3014–3023, 2018.
- [38] Anand Louis. Hypergraph markov operators, eigenvalues and approximation algorithms. In *Proceedings of the forty-seventh annual ACM symposium on Theory of computing*, pages 713–722, 2015.
- [39] Pedro Mercado, Francesco Tudisco, and Matthias Hein. Generalized matrix means for semi-supervised learning with multilayer graphs. In *Advances in Neural Information Processing Systems*, pages 14848–14857, 2019.
- [40] Elchanan Mossel and Jiaming Xu. Local algorithms for block models with side information. In *Proceedings of the 2016 ACM Conference on Innovations in Theoretical Computer Science*, pages 71–80, 2016.
- [41] Rafael Müller, Simon Kornblith, and Geoffrey E Hinton. When does label smoothing help? In *Advances in Neural Information Processing Systems*, pages 4696–4705, 2019.
- [42] Huda Nassar, Caitlin Kennedy, Shweta Jain, Austin R Benson, and David Gleich. Using cliques with higher-order spectral embeddings improves graph visualizations. In *Proceedings of The Web Conference 2020*, pages 2927–2933, 2020.
- [43] Quynh Nguyen, Francesco Tudisco, Antoine Gautier, and Matthias Hein. An efficient multilinear optimization framework for hypergraph matching. *IEEE transactions on pattern analysis and machine intelligence*, 39(6):1054–1075, 2016.
- [44] Ryan A Rossi, Nesreen K Ahmed, and Eunye Koh. Higher-order network representation learning. In *Companion Proceedings of the The Web Conference 2018*, pages 3–4, 2018.
- [45] Ryan A Rossi, Anup Rao, Sungchul Kim, Eunye Koh, Nesreen K Ahmed, and Gang Wu. Higher-order ranking and link prediction: From closing triangles to closing higher-order motifs. *arXiv preprint arXiv:1906.05059*, 2019.
- [46] Sai Nageswar Satchidanand, Harini Ananthapadmanaban, and Balaraman Ravindran. Extended discriminative random walk: a hypergraph approach to multi-view multi-relational transductive learning. In *Twenty-Fourth International Joint Conference on Artificial Intelligence*, 2015.
- [47] Nicholas D Sidiropoulos, Lieven De Lathauwer, Xiao Fu, Kejun Huang, Evangelos E Papalexakis, and Christos Faloutsos. Tensor decomposition for signal processing and machine learning. *IEEE Transactions on Signal Processing*, 65(13):3551–3582, 2017.
- [48] Christian Szegedy, Vincent Vanhoucke, Sergey Ioffe, Jon Shlens, and Zbigniew Wojna. Rethinking the inception architecture for computer vision. In *Proceedings of the IEEE conference on computer vision and pattern recognition*, pages 2818–2826, 2016.
- [49] Amanda L Traud, Peter J Mucha, and Mason A Porter. Social structure of facebook networks. *Physica A: Statistical Mechanics and its Applications*, 391(16):4165–4180, 2012.
- [50] Charalampos E Tsourakakis, Jakub Pachocki, and Michael Mitzenmacher. Scalable motif-aware graph clustering. In *Proceedings of the 26th International Conference on World Wide Web*, pages 1451–1460, 2017.
- [51] Nate Veldt, Austin R Benson, and Jon Kleinberg. Hypergraph cuts with general splitting functions. *arXiv preprint arXiv:2001.02817*, 2020.
- [52] Nate Veldt, Austin R Benson, and Jon Kleinberg. Localized flow-based clustering in hypergraphs. *arXiv preprint arXiv:2002.09441*, 2020.

- [53] Tao Wu, Austin R Benson, and David F Gleich. General tensor spectral co-clustering for higher-order data. In *Advances in Neural Information Processing Systems*, pages 2559–2567, 2016.
- [54] Han Xiao, Kashif Rasul, and Roland Vollgraf. Fashion-MNIST: a novel image dataset for benchmarking machine learning algorithms. *arXiv preprint arXiv:1708.07747*, 2017.
- [55] Lei Xu, Adam Krzyzak, and Ching Y Suen. Methods of combining multiple classifiers and their applications to handwriting recognition. *IEEE transactions on systems, man, and cybernetics*, 22(3):418–435, 1992.
- [56] Naganand Yadati, Madhav Nimishakavi, Prateek Yadav, Vikram Nitin, Anand Louis, and Partha Talukdar. Hypergcn: A new method for training graph convolutional networks on hypergraphs. In *Advances in Neural Information Processing Systems*, pages 1509–1520, 2019.
- [57] Hao Yin, Austin R Benson, Jure Leskovec, and David F Gleich. Local higher-order graph clustering. In *Proceedings of the 23rd ACM SIGKDD International Conference on Knowledge Discovery and Data Mining*, pages 555–564, 2017.
- [58] Muhan Zhang, Zhicheng Cui, Shali Jiang, and Yixin Chen. Beyond link prediction: Predicting hyperlinks in adjacency space. In *Thirty-Second AAAI Conference on Artificial Intelligence*, 2018.
- [59] Dengyong Zhou, Olivier Bousquet, Thomas N Lal, Jason Weston, and Bernhard Schölkopf. Learning with local and global consistency. In *Advances in neural information processing systems*, pages 321–328, 2004.
- [60] Dengyong Zhou, Jiayuan Huang, and Bernhard Schölkopf. Learning with hypergraphs: Clustering, classification, and embedding. In *Advances in neural information processing systems*, pages 1601–1608, 2007.
- [61] Xiaojin Zhu, Zoubin Ghahramani, and John D Lafferty. Semi-supervised learning using gaussian fields and harmonic functions. In *Proceedings of the 20th International conference on Machine learning (ICML-03)*, pages 912–919, 2003.
- [62] Xiaojin Zhu and Andrew B Goldberg. Introduction to semi-supervised learning. *Synthesis lectures on artificial intelligence and machine learning*, 3(1):1–130, 2009.

A Lemmas used in proofs

Lemma A.1. *Let $a, b, c > 0$. Then*

$$\log\left(\frac{a+c}{b+c}\right) \leq \frac{a}{a+c} \log\left(\frac{a}{b}\right)$$

Proof. Let $g(x) = x \log(x)$. We have

$$\frac{a+c}{b+c} \log\left(\frac{a+c}{b+c}\right) = g\left(\frac{a+c}{b+c}\right) = g\left(\frac{b}{b+c} \frac{a}{b} + \frac{c}{b+c}\right).$$

As $\frac{b}{b+c} + \frac{c}{b+c} = 1$ and g is convex, we can apply Jensen’s inequality to get

$$g\left(\frac{b}{b+c} \frac{a}{b} + \frac{c}{b+c}\right) \leq \frac{b}{b+c} g\left(\frac{a}{b}\right) + \frac{c}{b+c} g(1) = \frac{a}{b+c} \log\left(\frac{a}{b}\right).$$

Combining all together we get

$$\frac{a+c}{b+c} \log\left(\frac{a+c}{b+c}\right) \leq \frac{a}{b+c} \log\left(\frac{a}{b}\right)$$

which yields the claims. \square

Lemma A.2. *Assume that σ is one-homogeneous and positive and that both $y \in \mathbb{R}_{++}^n$ and $\alpha D_H^{-1/2} \mathcal{A}\sigma(D_H^{-1/2} f) + \beta D_G^{-1/2} A D_G^{-1/2} f \in \mathbb{R}_{++}^n$, for every $f \in \mathbb{R}_{++}^n$. Then*

$$\alpha D_H^{-1/2} \mathcal{A}\sigma(D_H^{-1/2} f) + \beta D_G^{-1/2} A D_G^{-1/2} f \leq C y$$

for all $f \in \mathbb{R}_{++}^n / \varphi$.

Proof. Since we are assuming that every node has hyper-degree $\delta_i = \sum_{jk} \mathcal{A}_{ijk} > 0$, for every i there exist j and k such that ijk is a hyperedge. Thus, if $U \subseteq V \times V$ is the set of nonzero entries of B , then $V \subseteq U$. Thus if $f > 0$ and $\varphi(f) = 1$ then f must be entrywise bounded. Hence, as φ is positive and one-homogeneous, we can choose

$$C = \frac{1}{\min_i y_i} \max_{i=1, \dots, n} \max_{f \in \mathbb{R}_{++}^n} \frac{(\alpha D_H^{-1/2} \mathcal{A}\sigma(D_H^{-1/2} f) + \beta D_G^{-1/2} A D_G^{-1/2} f)_i}{\varphi(f)} < +\infty$$

to obtain the claim. \square

Lemma A.3. Let $E : \mathbb{R}^n \rightarrow \mathbb{R}_+$ be defined by

$$E(f) = \frac{f^\top (D_H f - F(f))}{2} \quad (14)$$

with $F : \mathbb{R}^n \rightarrow \mathbb{R}^n$ differentiable and such that $F(f) \geq 0$ for all $f \geq 0$ and $F(\alpha f) = \alpha F(f)$ for all $\alpha \geq 0$. Then $\nabla E(f) = D_H f - F(f)$.

Proof. This is a relatively direct consequence of Euler's theorem for homogeneous functions. For completeness, we provide a self-contained proof here. Consider the function $G(\alpha) = F(\alpha f) - \alpha F(f)$. Then G is differentiable and $G(\alpha) = 0$ for all $\alpha \geq 0$. Thus, $G'(\alpha) = 0$ for all α in a neighborhood of $\alpha_0 = 1$. For any such α we have

$$G'(\alpha) = \alpha JF(\alpha f)f - F(f) = 0$$

where $JF(f)$ denotes the Jacobian of F evaluated at f . Evaluating G' on $\alpha = 1$ we get $JF(f)f = F(f)$. Therefore

$$2\nabla E(f) = \nabla \{f^\top (D_H f - F(f))\} = D_H f - F(f) + (D_H - JF(f))f = 2D_H f - 2F(f)$$

which gives us the claim. □